05,10

Hysteresis in magnetization curves of „ideal“ antiferromagnetic nanoparticles

© A.V. Lobachev, M.A. Chuev

National Research Center „Kurchatov Institute“ — Valiev Department of Physical and Technological Research, Moscow, Russia

E-mail: andrew_lv_91@mail.ru

Received October 11, 2025
Revised November 7, 2025
Accepted November 10, 2025

We have performed theoretical analysis of the magnetization curves of antiferromagnetic nanoparticles with „ideal“ shape for arbitrary orientation of the magnetic field relative to the axial magnetic anisotropy axis. It was found that the well-known values of critical magnetic fields for the longitudinal orientation of the magnetic field vector vary smoothly with increasing of angle between the field direction and the easy axis, such that the hysteresis loop width in the magnetization curves becomes narrower and disappears at a certain critical value of this angle. It was also shown that the hysteresis loop width and the critical angle itself increase with increasing ratio of the magnetic anisotropy constant to the exchange constant.

Keywords: magnetization curves, antiferromagnetic nanoparticles, hysteresis.

DOI: 10.61011/PSS.2025.11.62959.274-25

1. Introduction

In process of many years of fundamental research of structural, magnetic and thermodynamic characteristics of magnetic particles of small sizes (around several nanometers), a whole series of specific properties was found in these materials. This predetermined a wide area of their use in current nanotechnology. However, one of the most fundamental questions on the influence of magnetism nature in the materials that nanoparticles consist of on their essential characteristics still remains open to a large extent. For example, several models of antiferromagnetic (AFM) nanoparticles to describe their magnetization curves are actually based on the idea of a non-compensated spin in two magnetic sublattices introduced by Néel back in the beginning of the 60s in the last century [1]. Besides, from a thermodynamic point of view these models are reduced either to the corrections of the Langevin's function for anisotropy presence [2,3] or to the „nucleus-shell“ model to describe magnetization of nanoparticles [4] or to accounting for the dependence of magnetic torqie and antiferromagnetic susceptibility on temperature [5], or to the Heisenberg's model with account of anisotropy of individual ions and using Green's function [6].

The concept of the non-compensated spin is also actively used in the qualitative analysis of the experimental magnetization curves of AFM-nanoparticles [7–10]. Note also that to numerically describe the magnetic hysteresis in the experimental magnetization curves of iron borate, the approach based on the generalized Stoner–Wohlfarth model was used [11–13], and the antiferromagnetic nature of the studied material was taken into account as the additional contribution to Néel's magnetic susceptibility [14–16].

Despite the general validity of the Néel's physical idea as such [1], it played its negative role, too: the question on the shape of magnetization curves of ideal (compensated) AFM-nanoparticles since then has not been considered seriously, which, in its turn, held back the general theory development. It should be noted that recently the formalism was proposed and implemented to describe the specific transformation of Mössbauer spectra of absorption of ideal AFM-nanoparticles depending on temperature. The nontrivial shape of the energy spectrum of excitation of such particles made it possible to both describe the shape of the absorption spectra and give the phenomenological explanation of macroscopic quantum effects observed in the experiments [17]. At the same time it was shown that the presence of the non-compensated spin does not change the qualitative nature of evolution of the spectrum shape for „ideal“ antiferromagnetic particles with temperature, and results only to some quantitative corrections [18].

At the same time the hysteresis in an ideal antiferromagnetic was previously predicted also in the absence of the non-compensated spin back in the beginning of the 60s in the last century [19,20]. In particular, analytical equations were obtained for magnetization curves of a two-sublattice antiferromagnetic with weak magnetic anisotropy of „easy axis“ type for two mutually perpendicular orientations of the intensity vector of the external magnetic field **H** along and perpendicularly to the axis of anisotropy (see Figure 1). The energy density of such antiferromagnetic is expressed as follows:

$$E = J\mathbf{M}_1\mathbf{M}_2 - \frac{K}{2}(\cos^2\theta_1 + \cos^2\theta_2) - \mathbf{H}(\mathbf{M}_1 + \mathbf{M}_2), \quad (1)$$

where J — constant of exchange interaction ($J > 0$ for AFM particles), $\mathbf{M}_1$ and $\mathbf{M}_2$ — magnetizations of sublat-

tices ($M_1 = M_2 = M_0$), K — constant of axial magnetic anisotropy, θ_1 and θ_2 — angles between vectors $\mathbf{M}_1$ and $\mathbf{M}_2$ and easy magnetization axis.

When the external field is parallel to the easy magnetization axis ($\Theta = 0°$), magnetization curves are characterized by three values of critical fields:

$$h_\perp = \frac{2-k}{2+k} h_\parallel, \tag{2}$$

$$h_\parallel = \sqrt{k(2+k)}, \tag{3}$$

$$h_E(0) = 2 - k. \tag{4}$$

Here $k = K/(JM_0^2)$, and within the generally accepted (checked by experience for bulk AFM-materials [21]) assumption on the smallness of anisotropy energy compared to the exchange one $k \ll 1$. The equations (2)–(4) as such refer to a dimensionless magnetic field $h = H/(JM_0)$.

In the weak magnetic field (at $h \le h_\perp$) there is only one energy minimum, when magnetization vectors of sublattices $\mathbf{M}_1$ and $\mathbf{M}_2$ are parallel to the easy magnetization axis and antiparallel to each other, and the resulting magnetization is zero. In the field interval $h_\perp \le h \le h_\parallel$ the second energy minimum appears, besides, $M = 0$ still corresponds to the first minimum, whereas the one that corresponds to the second one is

$$M = 2M_0 h/h_E. \tag{5}$$

In this interval the scanning of magnetic field intensity first in ascending, and then in descending order (or vice versa) should lead to hysteresis in magnetization curves, if the relaxation processes (transitions between local energy minima) are rather slow. The physical meaning of indices $\parallel$ and $\perp$ consists in the fact that the axis of antiferromagnetism is perpendicular to the axis of anisotropy at $h \ge h_\perp$, and the situation when the axis of antiferromagnetism is parallel to the easy magnetization axis is implemented at $h \le h_\parallel$. Note that in the second case there are two equivalent solutions corresponding to permuation of $\mathbf{M}_1$ and $\mathbf{M}_2$ vector directions along the easy axis, whereas in the first case the solution is one, and it complies with the self-consistent precession of $\mathbf{M}_1$ and $\mathbf{M}_2$ vectors around the easy axis.

At $h > h_\parallel$ the energy minimum corresponding to $M = 0$ disappears, and only the second energy minimum stays, for which magnetization increases linearly with the magnetic field intensity increase according the law (5) to the value of $M = 2M_0$ at $h = h_E$. With further field increase magnetization stays unchanged, since its maximum value has already been achieved, corresponding to the orientation of $\mathbf{M}_1$ and $\mathbf{M}_2$ vectors along the field direction.

In case of perpendicular orientation of the magnetic field intensity vector relative to the easy axis ($\Theta = 90°$) there is only one critical field

$$h_E(90°) = 2 + k, \tag{6}$$

below which magnetization increases linearly from 0 to $2M_0$ (sublattice magnetization vectors, when the field increases from zero, immediately start turning towards the field direction), and above which the constant magnetization value is maintained, equal to $2M_0$.

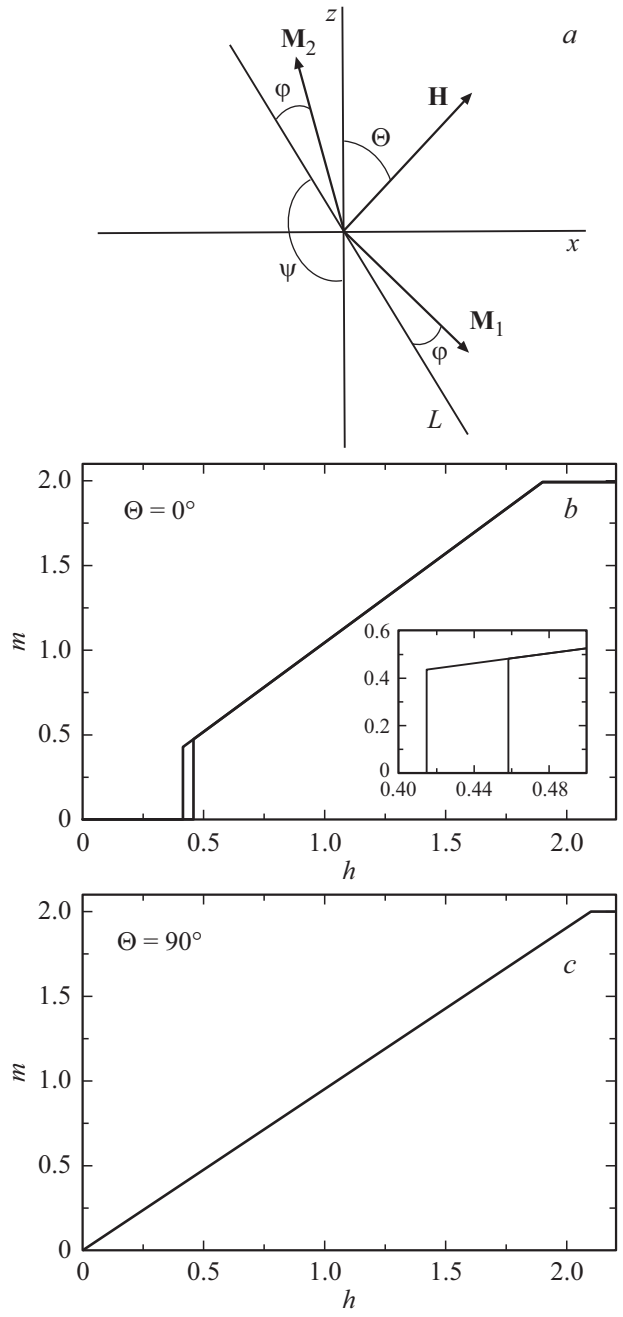

Figure 1. The system of coordinates: axis z — easy magnetization axis, L — antiferromagnetism axis (a). Magnetization curves at $\Theta = 0°$ (b) and $\Theta = 90°$ (c) at $k = 0.1$. Hereinafter $m = M/M_0$, the inserts show the curves on an enlarged scale.

Note that the analysis of the magnetization curve shape for arbitrary orientation of magnetic field direction relative to the anisotropy axis has not been done since. In this situation at least two questions arise: 1) how substantial is the accounting for the presence of hysteresis predicted for ideal AFM-nanoparticles, in the magnetization curves of real

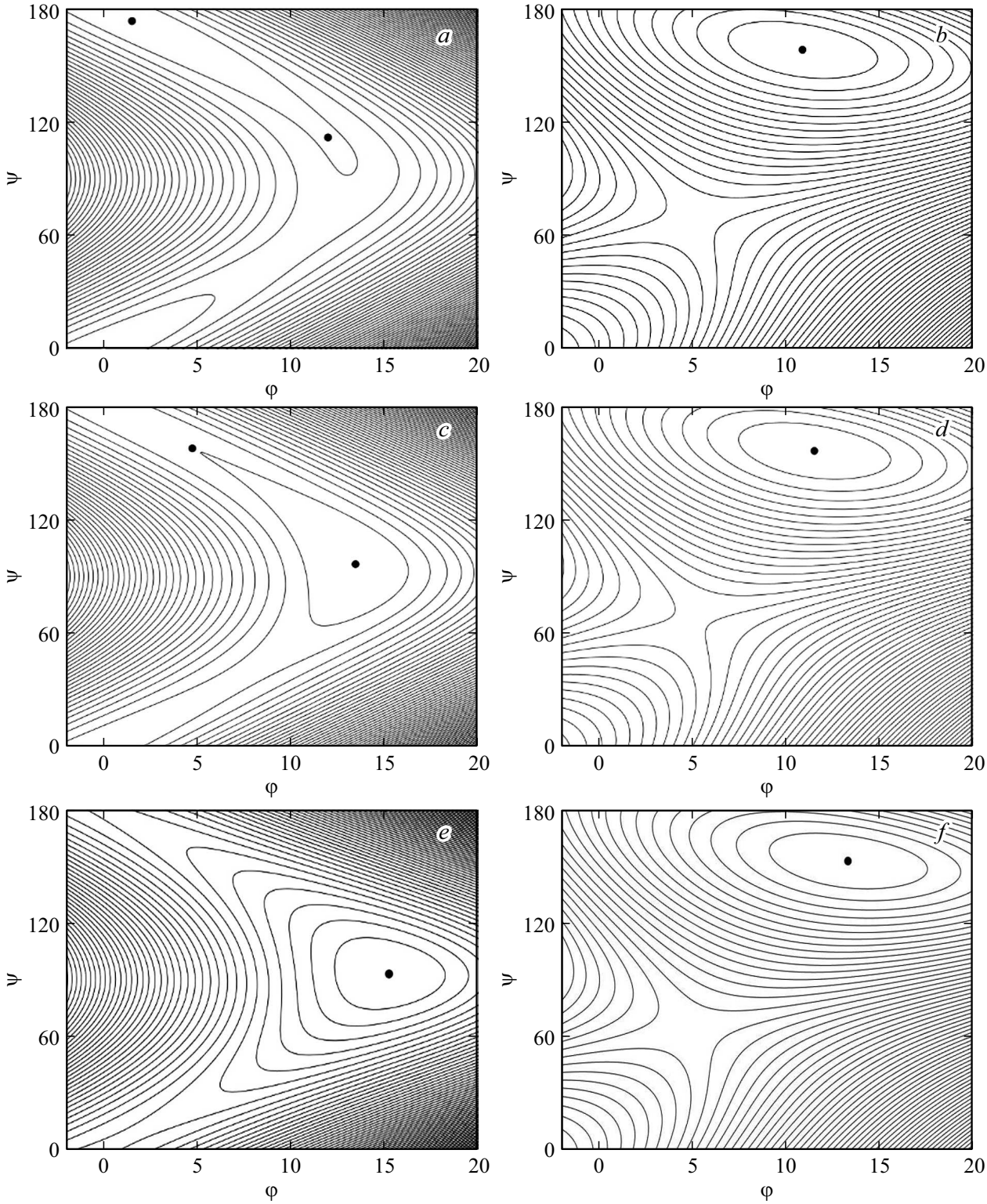

Figure 2. Constant energy level lines in φ and ψ variables for $\Theta = 1^\circ$ (a, c, e) and $\Theta = 45^\circ$ (b, d, f), calculated at $h = h_1(1^\circ)$ (a, b), $h_2(1^\circ)$ (c, d), 0.5 (e, f); $k = 0.1$. The points indicate the positions of local energy minima.

nanoparticles; 2) which effect is provided by orientation of magnetic field direction at the hysteresis value and shape for ideal AFM-nanoparticles. This article is dedicated to solving the corresponding problems, making it possible to clarify purely fundamental issues and to substantially expand the theoretical basis for development of adequate models to analyze multiple experimental data using state-of-the-art antiferromagnetic materials.

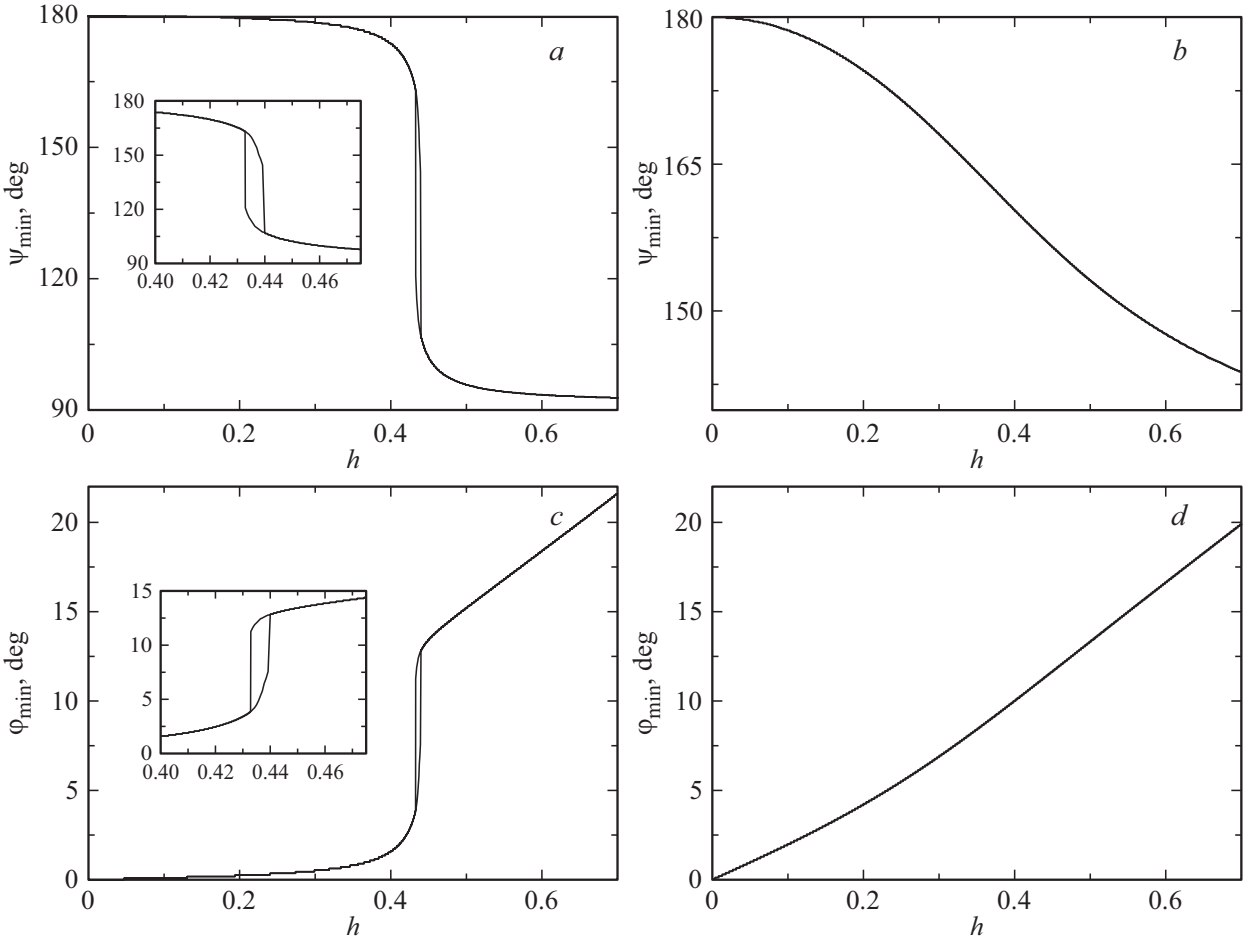

Figure 3. Dependences of coordinates of $\varphi_{\min}$ and $\psi_{\min}$ local energy minima on h magnetic field intensity for $\Theta = 2^\circ$ (a, c) and $45^\circ (b, d)$ calculated at $k = 0.1$.

To solve the problem of finding the energy minimum (1) it is convenient to change to new variables, angles φ and ψ (see Figure 1), and instead of energy (1) change to its normalized equation minus the minor constant summands [19,20]:

$$\widetilde{E} = 2\sin^2\varphi - k(2\sin^2\varphi\sin^2\psi - \sin^2\varphi - \sin^2\psi) - 2(h_z\sin\psi - h_x\cos\psi)\sin\varphi. \quad (7)$$

Here $\widetilde{E} = E/(JM_0^2) + 1 + k$, $h_z = h\cos\Theta$, $h_x = h\sin\Theta$. As in the case considered above $\Theta = 0^\circ$, potential energy minima must correspond to the system state (7). In Figure 2 we built the typical contour maps of constant energy levels in variables φ and ψ at $\Theta = 1^\circ$ and $\Theta = 45^\circ$ for different values of the magnetic field intensity module, the positions of local minima are indicated with points. Figure 3 shows the specific dependences of energy minima positions in variables φ and ψ on the magnetic field intensity for $\Theta = 2^\circ$ and $\Theta = 45^\circ$.

In weak magnetic fields $h \le h_1(\Theta)$ one energy minimum is implemented, when the sublattice magnetization vectors $\mathbf{M}_1$ and $\mathbf{M}_2$ deviate somewhat from the direction of the easy axis to the direction of the magnetic field staying almost antiparallel to each other (Figure 3). The antiferromagnetism vector also somewhat deviates from the easy axis direction, and the resulting non-zero magnetization occurs. If the condition $k \ll 1$ is met for small angles Θ, the second energy minimum appears in the field interval $h_1(\Theta) \le h \le h_2(\Theta)$ (Figure 2 and 3). Besides, almost antiparallel vectors of sublattice magnetization $\mathbf{M}_1$ and $\mathbf{M}_2$ still comply with the first minimum, being somewhat diverted from the axis of anisotropy, and the resulting magnetization is low. And the second minimum is characterized by the vector of antiferromagnetism, which is practially perpendicular to the axis of anisotropy, and vectors $\mathbf{M}_1$ and $\mathbf{M}_2$, which are almost antiparallel to each other, but are aligned nearly perpendicularly to the easy axis, so that the resulting magnetization approximately corresponds to equation (5). At $h \ge h_2(\Theta)$ only the second energy minimum remains. Such behavior is demonstrated graphically in Figure 2 and 3 on the left.

It is easy to understand that the critical fields $h_1(\Theta)$ and $h_2(\Theta)$ play a role of $h_\perp$ and $h_\parallel$ for the cases $\Theta > 0$, and the interval $h_1(\Theta) \le h \le h_2(\Theta)$ must show hysteresis loops in the magnetization curves.

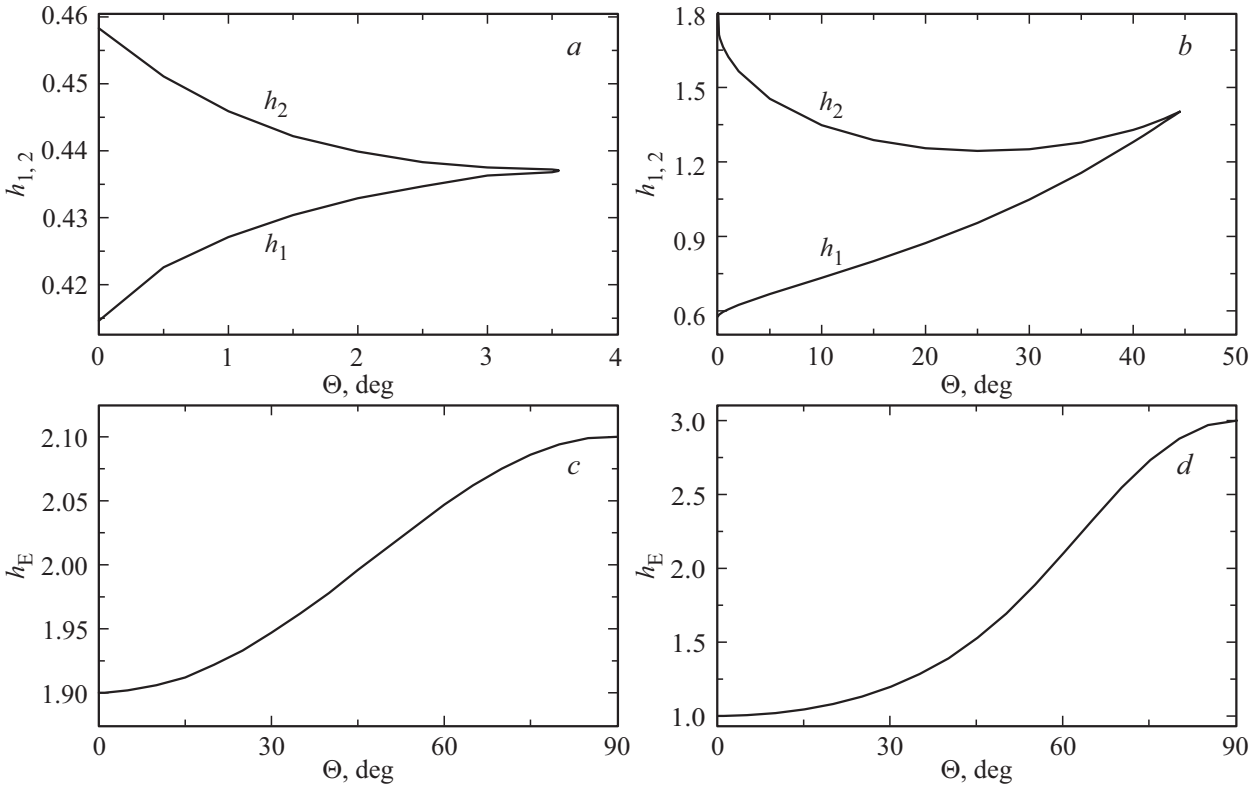

Figure 4. Dependence of critical magnetic fields on angle Θ for $k = 0.1$ (a, c) and 1 (b, d).

As you can see in the right parts in Figure 2 and 3, at $\Theta = 45^\circ$ only one energy minimum is always present in energy contour maps. This means that there is a certain critical angle with no hysteresis above. And indeed, on the left in Figure 4 there are charts of dependence of critical magnetic fields $h_1(\Theta)$ and $h_2(\Theta)$ on the angle Θ, calculated at $k = 0.1$. The area between $h_1(\Theta)$ and $h_2(\Theta)$ is exactly the area of hysteresis loops presence. From the upper chart you can see that as Θ increases, the hysteresis area becomes narrower and narrower, and at $\Theta_C = 3.55^\circ$ hysteresis fully disappears. Similarly to the case $\Theta = 0^\circ$, there shall be another critical field $h_E(\Theta)$, above which vectors $\mathbf{M}_1$ and $\mathbf{M}_2$ become parallel, so that at $h \geq h_E(\Theta)$ the constant value of resulting magnetization equal to $2M_0$ is maintained. The lower chart in Figure 4 shows the dependence of the third critical field h_E on angle Θ. From this chart you can see that as Θ grows from 0 to 90°, the h_E value gradually rises from $2 - k$ to $2 + k$. At the same time for $k \ll 1$ this dependence is described with equation

$$h_E(\Theta) \approx 2 - k \cos 2\Theta. \tag{8}$$

The positions of local energy minima in φ and ψ coordinates obtained within the completed calculations may be used to calculate the magnetization curves of ensembles of ideal AFM-particles with the specified angle Θ:

$$m(\Theta, h) = 2 \sin \varphi_{\min} (\sin \Psi_{\min} \cos \theta - \cos \Psi_{\min} \sin \theta). \tag{9}$$

At the same time the magnetization curves of the ensemble of chaotically oriented AFM-particles are described by the standard equation

$$m(h) = \int_0^{\pi/2} m(\Theta, h) \sin \Theta \, d\Theta. \tag{10}$$

Figure 5 on the left presents the magnetization curves for groups of AFM particles with the specified values $\Theta = 2, 45, 80^\circ$ and for the ensemble of chaotically oriented AFM-nanoparticles calculated at $k = 0.1$. The hysteresis loop is only observed in the magnetization curve at small angle $\Theta = 2^\circ$ and is absent in other curves. This circumstance results in the fact that in the integral curve for the ensemble of chaotically oriented AFM-particles the hysteresis is practically unseen. In fact, this result means that if you stay within the generally accepted assumption on smallness of anisotropy energy compared to the exchange one $(k \ll 1)$, hysteresis in the experimental magnetization curves of AFM-particles may be explained exclusively by the presence of the non-compensated magnetic torque.

However, a successful numerical analysis has been conducted recently on the experimental data measured on hematite nanoparticles [22–24] within the continual model of magnetic dynamics of the ensemble of ideal AFM-nanoparticles in the two-sublattice approximation [17]. And this analysis was based on a totally different qualitative assumption that the decisive factor for the magnetic effects

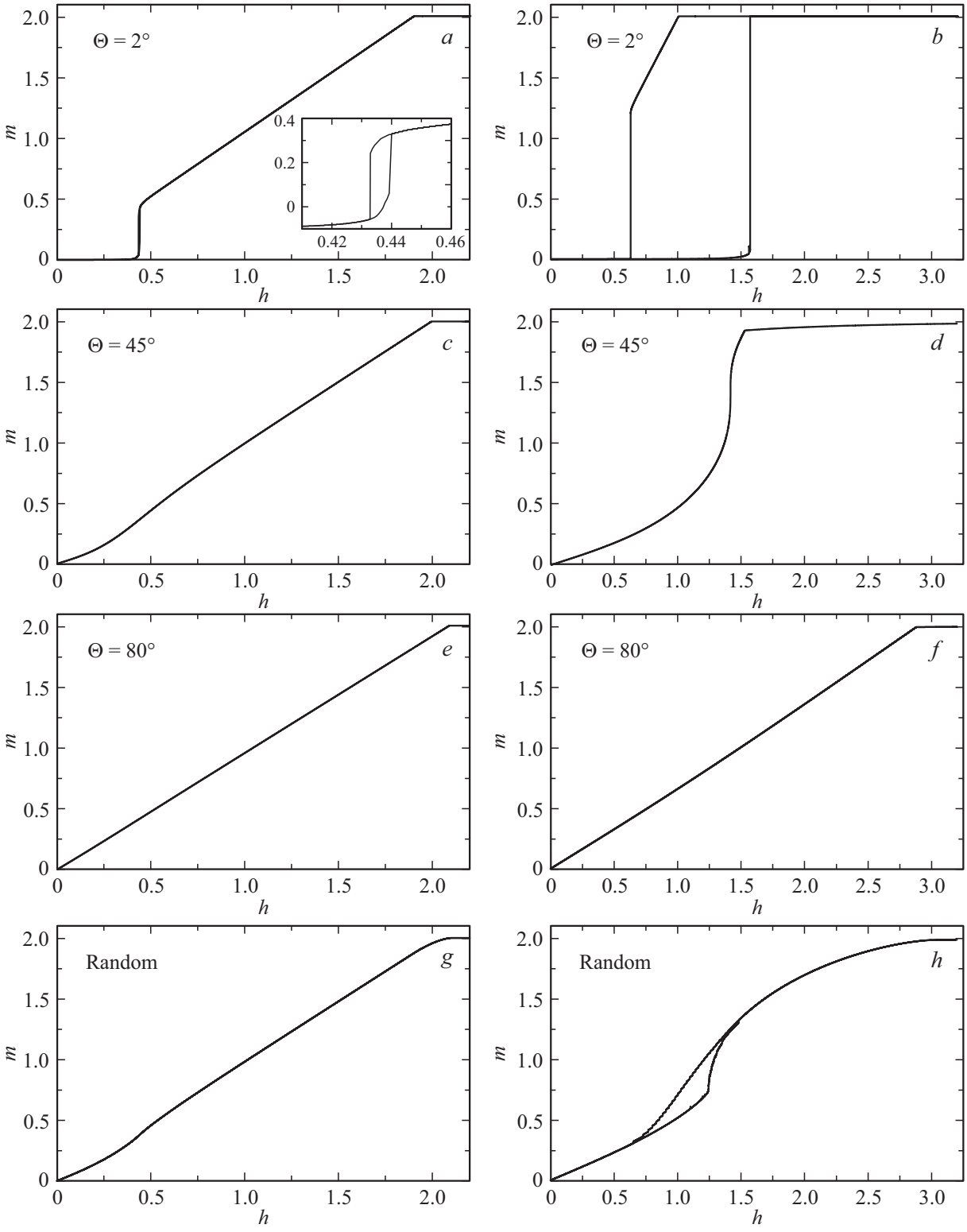

Figure 5. Magnetization curves for groups of particles with different angles Θ and ensemble of chaotically oriented antiferromagnetic nanoparticles calculated at $k = 0.1$ (a, c, e, g) and 1 (b, d, f, h).

in AFM-nanoparticles is not the presence of the non-compensated spin, but cardinal increase of anisotropy of the particle shape with the decrease in the particle size, which causes increase of k and chaotic orientation of the axes of the resulting magnetic anisotropy relative to the crystallographic axes. In this situation the condition $k \ll 1$ will no longer be met, and hysteresis loops in the magnetization curves of AFM-nanoparticles may take absolutely

different shapes (see, for example, [25]). And the general statement is such that with growth of k the hysteresis loop should broaden, and in the limiting case $k \gg 1$, when the exchange interaction becomes rather weak, it shall acquire ferromagnetic nature [11].

Let us also note that in the limiting case of weak magnetic fields $h \ll 1$ you can obtain the approximated equations for the functional dependence of magnetization of groups of nanoparticles with small angle $\Theta \ll 1$ with the precision of up to linear members at h

$$m(\Theta, h) \approx \frac{2h \sin^2 \Theta}{2 + k} \tag{11}$$

and the corresponding equations for the groups of nanoparticles with small values of angle deviation Θ on 90°, $\pi/2 - \Theta \ll 1$

$$m(\Theta, h) \approx \frac{h \sin 2\Theta}{2 - k}. \tag{12}$$

The detailed analysis of the shape of magnetization curves depending on k, in particular, for $k \geq 1$ is outside the framework of this article. However, we calculated the dependences of the critical magnetic fields on angle Θ for $k = 1$ (Figure 4, on the right) and magnetization curves for the groups of AFM-particles with different angles Θ and the ensemble of chaotically oriented AFM-nanoparticles for $k = 1$ (Figure 5, on the right). As you can see in these figures, the interval of angles Θ, at which hysteresis is observed, increased significantly ($\Theta_C = 45°$ for $k = 1$), and the width of the hysteresis loops for different Θ increased substantially compared to the case of $k = 0.1$. These effects result in the fact that the hysteresis loop in the resulting magnetization curve for the ensemble of the chaotically oriented AFM-particles with $k = 1$ acquires a rather distinct shape.

To conclude, note that this paper contains the numerical analysis of the shape of magnetization curves of „ideal" antiferromagnetic nanoparticles in the two-sublattice approximation for the random orientation of the magnetic field direction along the axis of the axial magnetic anisotropy. For the first time the dependences of critical magnetic field intensities on the magnetic field vector orientation were built, which vary gradually with the increase of the angle between the field direction and the easy axis. It was found that the width of the hysteresis loops in the magnetization curves narrows with the growth of this angle and disappears at its certain critical value. It was also shown that the width of the hysteresis loop and the critical angle as such grow with the increase of the ratio of the magnetic anisotropy constant to the exchange constant. The fundamental nature of these results makes it possible to qualitatively explain the features observed in the experimental magnetization curves, and also serve as the basis for the development of more adequate theoretical models to describe the experimental data.

The results obtained in this paper may easily be generalized for the case of the presence of non-compensated spin in AFM-particles, which will make it possible to include two mutually competing mechanisms of hysteresis loop formation in the model for description of magnetization curves, and therefore to expand substantially the theoretical basis for the development of the experimental data analysis methods.

Funding

The study was performed under the State assignment of National Research Center „Kurchatov Institute".

Conflict of interest

The authors declare that they have no conflict of interest.

References

[1] L. Néel. C.R. Acad. Sci. Paris **252**, 4075 (1961); **253**, 9 (1961); **253**, 203 (1961); **253**, 1286 (1961).
[2] C. Gilles, P. Bonville, K.K.W. Wong, S. Mann. Eur. Phys. J. B **17**, 417 (2000).
[3] Yu.L. Raykher, V.I. Stepanov, S.V. Stolyar, V.P. Ladygina, D.A. Balaev, L.A. Ischenko, M. Balashoyu. FTT **52** (in Russian), *2*, 277 (2010).
[4] R. Bhowmik, R. Nagarajan, R. Ranganathan. Phys. Rev. B **69**, 054430 (2004).
[5] D.E. Madsen, S. Mørup, M.F. Hansen. J. Magn. Magn. Mater. **305**, 95 (2006).
[6] J.M. Wesselinowa. J. Magn. Magn. Mater. **322**, 234 (2010).
[7] F. Bødker, M.F. Hansen, C.B. Koch, K. Lefmann, S. Mørup. Phys. Rev. B **61**, 6826 (2000).
[8] O. Ozdemir, D.J. Dunlop, T.S. Berquo. Geochem. Geophys. Geosyst. **9**, 10 (2008).
[9] A.H. Hill, F. Jiao, P.G. Bruce, A. Harrison, W. Kockelmann, C. Ritter. Chem. Mater. **20**, 4891 (2008).
[10] G.C. Papaefthymiou. Biochim. Biophys. Acta **1800**, 886 (2010).
[11] M.A. Chuev, J. Hesse, J. Phys. Condens. Matter **19**, 506201 (2007).
[12] D.L. Zagorsky, K.V. Frolov, S.A. Bedin, I.V. Perunov, A.A. Lomov, M.A. Chuev, I.M. Doludenko. FTT **60**, *11*, 2075 (2018). (in Russian).
[13] D.L. Zagorskiy, I.M. Doludenko, K.V. Frolov, I.V. Perunov, M.A. Chuev, N.K. Chumakov, I.V. Kalachikova, V.V. Artyomov, T.V. Tsyganova, S.S. Kruglikov. FTT **65**, *6*, 973 (2023). (in Russian).
[14] N.I. Snegiryov, I.S. Lyubutin, S.V. Yagupov, M.A. Chuev, N.K. Chumakov, O.M. Zhigalina, D.N. Khmelenin, M.B. Strugatskiy. ZhNKh **66**, *8*, 1114 (2021). (in Russian).
[15] M.A. Chuev. Proc. SPIE **12157**, 121571C (2022).
[16] A.P. Nosov, I.A. Subbotin, M.A. Chuev, A.O. Belyaeva, O.A. Kondratiev, E.A. Ganshina, I.M. Pripechenkov, S.S. Dubinin, A.O. Shorikov, V.V. Izyurov, K.A. Merentsova, M.S. Artemiev, E.M. Pashaev. FMM **126**, *5*, 520 (2025). (in Russian).
[17] M.A. Chuev. Pisma v ZhETF **95**, *6*, 323; **103**, *3*, 194 (2016). (in Russian)

[18] M.A. Chuev. DAN **447**, *1*, 22 (2012). (in Russian).
[19] E.A. Turov. V sb.: Ferromagnitnyi rezonans / Pod red. S.V. Vonsovskogo. Fizmatlit, M. (1961). S. 98. (in Russian).
[20] S.V. Vonsovsky. Magnetizm. Nauka, M. (1971). 1032 s. (in Russian).
[21] I.E. Dzyaloshinski, ZhETF **32**, *6*, 1547 (1957). (in Russian).
[22] I. Mischenko, M. Chuev. Hyperfine Interact. **237**, 21 (2016).
[23] M.A. Chuev, I.N. Mischenko, S.P. Kubrin, T.A. Lastovina. Pisma v ZhTF **105**, *11*, 668 (2017). (in Russian).
[24] I. Mishchenko, M. Chuev, S. Kubrin, T. Lastovina,V. Polyakov, A. Soldatov. J. Nanoparticle Res. **20**, 141 (2018).
[25] A.K. Zvezdin, M.A. Kolyushenkov, A.P. Pyatakov. Pisma v ZhETF **121**, *7*, 605 (2025). (in Russian) .

Translated by M.Verenikina